

Reactivity of the Ruthenium Hydride Complex [Ru{ κ^3 -H,S,S-HB(mt)₃}H(PPh₃)₂] (HB(mt)₃ = hydrotris(methimazolyl)borate): Catalytic Dimerization of 1-Alkynes and Proton Transfer Reactions

Manuel Jiménez-Tenorio, M. Carmen Puerta,* and Pedro Valerga*

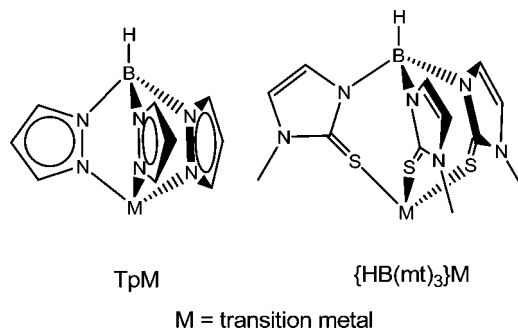
Departamento de Ciencia de Materiales e Ingeniería Metalúrgica y Química Inorgánica, Facultad de Ciencias, Universidad de Cádiz, 11510 Puerto Real, Cádiz, Spain

Received February 27, 2009

The complex [Ru{ κ^3 -H,S,S-HB(mt)₃}H(PPh₃)₂] (**1**, HB(mt)₃ = hydrotris(methimazolyl)borate; mt = *N*-methyl-2-mercaptoimidazolyl) containing a three-center two-electron Ru–H–B bonding interaction has been prepared by reaction of [RuHCl(PPh₃)₃] with Na[HB(mt)₃] in MeOH at 40 °C. This compound, which occurs in solution as a mixture of two stereoisomers (**1a** and **1b**), has been spectroscopically and structurally characterized. **1** reacts over a two-day period with CH₂Cl₂/MeOH at room temperature, furnishing the methimazolate complex [RuH(mt)(PPh₃)₃] (**2**). The latter compound exists in solution as a 55:45 mixture of stereoisomers, and they were structurally characterized. Both **1** and **2** are catalyst precursors for the dimerization of 1-alkynes (toluene, 85 °C, 2% catalyst load) to mixtures of *Z*, *E*, and *gem*-stereoisomers of the corresponding enynes. Compound **1** is much more active and selective than **2**. In the presence of benzoic acid, the activity of the catalyst decreases, but the stereoselectivity toward the (*Z*)-enynone isomer increases. NMR monitoring of the reaction of **1** with PhCOOH in CD₂Cl₂ in the temperature range –60 to 0 °C has allowed the identification of what seems to be a dihydrogen-bonded complex between the stereoisomer **1b** and PhCOOH. This species exhibits a very short minimum longitudinal relaxation time of 5.9 ms. Protonation of **1** with HBF₄·OEt₂ in CD₂Cl₂ at –60 °C yields the metastable dihydrogen complex [Ru{ κ^3 -H,S,S-HB(mt)₃}H₂(PPh₃)₂][BF₄] (**3a**), which loses H₂ as the temperature increases, furnishing the complex [Ru{ κ^3 -H,S,S-HB(mt)₃}H(PPh₃)₂][BF₄], which is most likely coordinatively unsaturated. Likewise, the protonation of **2** with HBF₄·OEt₂ in CD₂Cl₂ at –60 °C generates the dihydrogen complex [Ru(mt)(H₂)(PPh₃)₃][BF₄] (**4**) as a 5:1 mixture of two stereoisomers.

Introduction

Since its introduction by Reglinski and Spicer, the hydrotris(methimazolyl)borate anion ([HB(mt)₃][–], mt = *N*-methyl-2-mercaptoimidazolyl) has been regarded as the soft donor atom equivalent of the N-donor anion hydrotris(pyrazolyl)borate (Tp).¹



Formally, both HB(mt)₃ and Tp present analogies, which anticipate similar stoichiometries for their complexes with transition metals. However, there are also noticeable differences in the chemical behavior, not only resulting from the electronic

capabilities of the S- or N-donor atoms but also due to the different conformational nature of the rings in the HB(mt)₃-metal or Tp-metal cages.^{2–12} Thus, complexation by the three nitrogen atoms of the Tp ligand (κ^3 -N,N,N) provides a bicy-

(2) Bailey, P. J.; Lorono-Gonzales, D. J.; McCormack, C.; Parsons, S.; Price, M. *Inorg. Chim. Acta* **2003**, *354*, 61–67.

(3) Kuan, S. L.; Leong, W. K.; Goh, L. Y.; Webster, R. D. *Organometallics* **2005**, *24*, 4639–4648.

(4) Kuan, S. L.; Leong, W. K.; Goh, L. Y.; Webster, R. D. *J. Organomet. Chem.* **2006**, *691*, 907–915.

(5) Bailey, P. J.; Dawson, A.; McCormack, C.; Moggach, S. A.; Oswald, I. D. H.; Parsons, S.; Rankin, D. W. H.; Turner, A. *Inorg. Chem.* **2005**, *44*, 8884–8898.

(6) Bailey, P. J.; McCormack, C.; Parsons, S.; Rudolphi, F.; Sánchez Perucha, A.; Wood, P. *Dalton Trans.* **2007**, 476–480.

(7) Hill, A. F.; Owen, G. R.; White, A. J. P.; Williams, D. J. *Angew. Chem., Int. Ed.* **1999**, *38*, 2759–2761.

(8) Foreman, M. R.; St, J.; Hill, A. F.; Owen, G. R.; White, A. J. P.; Williams, D. J. *Organometallics* **2003**, *22*, 4446–4450.

(9) Abernethy, R. J.; Hill, A. F.; Tshabang, N.; Willis, A. C.; Young, R. D. *Organometallics* **2009**, *28*, 488–492.

(10) (a) Buccella, D.; Shultz, A.; Melnick, J. G.; Konopka, F.; Parkin, G. *Organometallics* **2006**, *25*, 5496–5499. (b) Bridgewater, B. M.; Parkin, G. *J. Am. Chem. Soc.* **2000**, *122*, 7140–7141. (c) Kimblin, C.; Bridgewater, B. M.; Hascall, T.; Parkin, G. *J. Chem. Soc., Dalton Trans.* **2000**, 891–897.

(11) (a) Garner, M.; Lehmann, M.; Reglinski, J.; Spicer, M. D. *Organometallics* **2001**, *20*, 5233–5236. (b) Ojo, J. F.; Slavin, P. A.; Reglinski, J.; Spicer, M. D.; Garner, M.; Kennedy, A. R.; Teat, S. J. *Inorg. Chim. Acta* **2001**, *313*, 15–20.

(12) Patel, D. V.; Mihalcik, D. J.; Kreisel, K. A.; Yap, G. P. A.; Zakharov, L. N.; Kassel, W. S.; Rheingold, A. L.; Rabinovich, D. J. *Chem. Soc., Dalton Trans.* **2005**, 2410–2416.

* To whom correspondence should be addressed. E-mail: carmen.puerta@uca.es; pedro.valerga@uca.es. Tel: +34 956 016350. Fax: +34 956 016288.

(1) Reglinski, J.; Garner, M.; Cassidy, I. D.; Slavin, P. A.; Spicer, M. D.; Armstrong, D. R. *J. Chem. Soc., Dalton Trans.* **1999**, 2119–2126.

clo[2.2.2] cage containing six-membered rings, whereas the HB(mt)₃ ligand forms eight-membered rings when bound through its three sulfur atoms to the metal (κ^3 -S,S,S), resulting in a bicyclo[3.3.3] cage.⁵ One important consequence is that κ^3 -S,S,S-HB(mt)₃ complexes potentially display a novel form of atropisomerism in which rotation is restricted about a three-dimensional cage rather than about a single bond.⁶ Several ruthenium complexes containing the HB(mt)₃ ligand bound in a κ^3 -S,S,S fashion have been reported.^{2–6} One important feature of the HB(mt)₃ ligand observed in some ruthenium complexes is the ability of binding by means of a B–H–Ru three-center two-electron bonding.^{3,4,7–9} This results in a κ^3 -H,S,S coordination mode that involves the formation of a bicyclo[1.3.3] cage, as in the case of the complex [Ru{ κ^3 -H,S,S-HB(mt)₃}H(CO)-(PPh₃)].⁸ This more compact arrangement seems to be preferred under certain circumstances to the geometrical constraints imposed by the bicyclo[3.3.3] unit in the κ^3 -S,S,S coordination mode. When bound in this fashion, the HB(mt)₃ ligand in [Ru{ κ^3 -H,S,S-HB(mt)₃}H(CO)(PPh₃)] undergoes a thermal dehydrogenation, which involves intramolecular BH activation. This process leads to the remarkably stable ruthenaboratrane complex [Ru{ κ^3 -S,S,S-B(mt)₃}H(CO)(PPh₃)], which contains a ruthenium to boron dative bond.⁷ The homologous osmaboratrane complex [Os{ κ^3 -S,S,S-B(mt)₃}H(CO)(PPh₃)] has been also reported.¹³ The ruthenaboratrane complex [Ru(κ^3 -S,S,S-B(mt)₃)(CO)(PPh₃)] is also readily generated by elimination of RH from [Ru{ κ^3 -H,S,S-HB(mt)₃}R(CO)(PPh₃)] (R = CH=CH₂, CH=CHCPh₂(OH), CH=CH(4-MeC₆H₄), C₆H₅) upon BH activation. [Ru{ κ^3 -S,S,S-B(mt)₃}H(CO)(PPh₃)] is rather inert once formed and does not react with H₂ at ambient temperatures and pressures to re-form [Ru{ κ^3 -H,S,S-HB(mt)₃}H(CO)(PPh₃)].^{7,8} Furthermore, the reaction of [Ru{ κ^3 -H,S,S-HB(mt)₃}H(CO)-(PPh₃)] with PhC≡CH in dichloromethane leads to the quantitative formation of styrene and [Ru{ κ^3 -S,S,S-B(mt)₃}H(CO)(PPh₃)] over a period of 23 h at room temperature.⁸ No alkyne coupling products have been observed in this process, most likely due to the robust nature of the ruthenaboratrane complex.

Our research group has been studying for some time the chemistry of ruthenium complexes bearing hydrotris(pyrazolyl)borate and phosphine ligands.^{14–18} We have developed a number of catalytic application with these complexes to processes such as alkyne coupling reactions,¹⁵ synthesis of enolactone,¹⁶ or enantioselective solvent-free cycloaddition reactions.¹⁸ Given the versatility of the coordination modes for the HB(mt)₃ ligand, we became interested in testing the ability of ruthenium complexes bearing this ligand as catalyst precursors in alkyne coupling reactions. Given the fact that no catalytic activity toward PhC≡CH has been reported for [Ru{ κ^3 -H,S,S-HB(mt)₃}H(CO)(PPh₃)],⁸ we decided to avoid the use of CO, replacing it with PPh₃. Rather unexpectedly, we have found that the resulting complex [Ru{ κ^3 -H,S,S-HB(mt)₃}H(PPh₃)₂] (**1**) is catalytically active for the dimerization of 1-alkynes. This is only the second example of a catalytic process effected by methimazolylborate complexes.^{10a} The ruthenaboratrane com-

plex [Ru{ κ^3 -S,S,S-B(mt)₃}H(PPh₃)₂] has not been observed in our system. It seems as if the CO ligand strongly contributes to the stabilization of the ruthenaboratrane species. In this work we describe the preparation, structural characterization, and chemical properties of [Ru{ κ^3 -H,S,S-HB(mt)₃}H(PPh₃)₂], its catalytic activity toward the dimerization of 1-alkynes, and a NMR study of its protonation reactions.

Experimental Section

All synthetic operations were performed under a dry dinitrogen or argon atmosphere following conventional Schlenk techniques. Tetrahydrofuran, diethyl ether, and petroleum ether (boiling point range 40–60 °C) were obtained oxygen- and water-free from an Innovative Technology, Inc. solvent purification apparatus. Other solvents (toluene, dichloromethane, methanol) were of anhydrous quality and used as received. All solvents were deoxygenated immediately before use. The ligand sodium tris(methimazolyl)borate (Na[HB(mt)₃]) was prepared following suitable adaptations of published procedures.^{1,2} [RuHCl(PPh₃)₃] was prepared by a modified procedure developed in our laboratory.¹⁹ Reaction of HBF₄·OEt₂ and benzoic acid were used as supplied by Aldrich. IR spectra were taken in Nujol mulls on a Perkin-Elmer Spectrum 1000 FTIR spectrophotometer. NMR spectra were taken on a Varian Unity 400 MHz or Varian Gemini 300 MHz equipment. Chemical shifts are given in ppm from SiMe₄ (¹H and ¹³C{¹H}), 85% H₃PO₄ (³¹P{¹H}), or BF₃·OEt₂ (¹¹B). Longitudinal relaxation times (*T*₁) measurements were made by the inversion–recovery method. Microanalysis was performed on an elemental analyzer model LECO CHNS-932 at the Servicio Central de Ciencia y Tecnología, Universidad de Cádiz.

[Ru{ κ^3 -H,S,S-HB(mt)₃}H(PPh₃)₂], **1**. To a slurry of [RuHCl(PPh₃)₃] (0.47 g, 0.5 mmol) in methanol (10 mL) was added sodium hydrotris(methimazolyl)borate (Na[HB(mt)₃]), 0.2 g, ca. 0.5 mmol). The mixture was stirred in a water bath at 45 °C for 30 min. The color of the mixture changed gradually from purple to yellow, and a microcrystalline yellow precipitate was formed. The precipitate was filtered off, washed with ethanol and petroleum ether, and dried in vacuo. The resulting material is a mixture of two diastereoisomers. It was recrystallized by dissolving the crude product in hot toluene, filtering the solution, and layering with diethyl ether. Greenish-yellow crystals were obtained, containing one toluene molecule of crystallization. Yield: 0.4 g, 75%. Anal. Calcd for C₄₈H₄₇N₆BP₂RuS₃·C₇H₈: C, 61.7; H, 5.18; N, 7.9. Found: C, 61.4; H, 5.01; N, 8.1. IR: ν (RuH) 2012, ν (BH) 2170 cm⁻¹. The product exists in solution as a mixture of two stereoisomers, **1a** and **1b**, present in variable amounts depending on the solvent. NMR data for isomer **1a** in CD₂Cl₂ (relative amount 64%): ¹H NMR (400 MHz, CD₂Cl₂, 298 K): δ -17.68 (t, ²*J*_{HP} = 27.7 Hz, 1 H, RuH), -3.89 (m br, 1 H, RuHB), 3.04 (s, 6 H, NCH₃ of coordinated methimazolate rings), 3.65 (s, 3 H, NCH₃ of uncoordinated methimazolate ring), 6.38, 6.77 (d, ³*J*_{HH} = 2.2 Hz, 1 H each, CHCH of uncoordinated methimazolate ring), 6.48, 6.68 (d, ³*J*_{HH} = 1.9 Hz, 2 H each, CHCH of coordinated methimazolate rings), 6.91–7.49 (m, 30 H, P(C₆H₅)₃). ³¹P{¹H} NMR (161.89 MHz, CD₂Cl₂, 298 K): δ 63.8 (s). ¹³C{¹H} NMR (101 MHz, CD₂Cl₂, 298 K): δ 34.26 (NCH₃ of coordinated methimazolate rings); 35.04 (s, NCH₃ of uncoordinated methimazolate ring); 118.30, 120.26 (s, CHCH of uncoordinated methimazolate ring); 119.15, 119.66 (s, CHCH of coordinated methimazolate rings); 126.82, 127.92, 129.3, 134.86 (s, P(C₆H₅)₃); 166.1, 166.5 (s, C=S). ¹¹B NMR (128 MHz, CD₂Cl₂, 298 K): 1.6 (br). NMR data for isomer **1b** in CD₂Cl₂ (relative amount 36%): ¹H NMR (400 MHz, CD₂Cl₂, 298 K): δ -12.35 (t, ²*J*_{HP} = 24.3 Hz, 1 H, RuH), -8.11 (m br, 1 H, RuHB),

(13) Foreman, M. R. St.-J.; Hill, A. F.; White, A. J. P.; Williams, D. J. *Organometallics* **2004**, *23*, 913–916.

(14) Jiménez-Tenorio, M. A.; Jiménez-Tenorio, M.; Puerta, M. C.; Valerga, P. *Inorg. Chim. Acta* **1997**, *259*, 77–84.

(15) Jiménez-Tenorio, M. A.; Jiménez-Tenorio, M.; Puerta, M. C.; Valerga, P. *Organometallics* **2000**, *19*, 1333–1342.

(16) Jiménez-Tenorio, M.; Puerta, M. C.; Valerga, P.; Moreno-Dorado, F. J.; Guerra, F. M.; Massanet, G. M. *Chem. Commun.* **2001**, 2324–2325.

(17) Jiménez-Tenorio, M.; Palacios, M. D.; Puerta, M. C.; Valerga, P. *Organometallics* **2005**, *24*, 3088–3098.

(18) Jiménez-Tenorio, M.; Palacios, M. D.; Puerta, M. C.; Valerga, P. *J. Mol. Catal. A: Chem.* **2007**, *261*, 64–72.

(19) Jiménez-Tenorio, M.; Puerta, M. C.; Valerga, P. *Inorg. Chem.* **1994**, *33*, 3515–3520.

3.26, 3.31, 3.53 (s, 3 H each, NCH₃ of methimazole rings), 5.94, 6.20, 6.52, 6.55, 6.58, 6.66 (s br, 1 H each, CH of methimazole rings), 6.91–7.49 (m, 30 H, P(C₆H₅)₃). ³¹P{¹H} NMR (161.89 MHz, CD₂Cl₂, 298 K): δ 61.3 (d, ²J_{PP} = 36 Hz), 73.6 (br). ¹³C{¹H} NMR (101 MHz, CD₂Cl₂, 298 K): δ 34.37, 34.57, 34.92 (NCH₃); 117.60, 118.46, 118.64, 119.05, 119.82, 120.1 (s, CH of methimazole ring); 127.03, 127.11, 127.75, 128.55, 128.48, 134.28 (P(C₆H₅)₃); 165.5, 166.0, 166.5 (s, C=S). ¹¹B NMR (128 MHz, CD₂Cl₂, 298 K): 0.7 (br). NMR data for isomer **1a** in C₂D₂Cl₄ (relative amount 100%): ¹H NMR (400 MHz, C₂D₂Cl₄, 298 K): δ -17.51 (t, ²J_{HP} = 27.6 Hz, 1 H, RuH), -4.50 (br, 1 H, RuHB), 2.63 (s, 6 H, NCH₃ of coordinated methimazole rings), 3.23 (s, 3 H, NCH₃ of uncoordinated methimazole ring), 5.84, 6.26 (d, ³J_{HH} = 2.2 Hz, 1 H each, CHCH of uncoordinated methimazole ring), 6.06, 6.31 (d, ³J_{HH} = 1.9 Hz, 2 H each, CHCH of coordinated methimazole rings), 6.55, 6.68, 6.97 (m, 30 H, P(C₆H₅)₃). ³¹P{¹H} NMR (161.89 MHz, C₂D₂Cl₄, 298 K): δ 63.0 (s). ¹³C{¹H} NMR (101 MHz, C₂D₂Cl₄, 298 K): δ 32.86 (NCH₃ of coordinated methimazole rings); 33.86 (s, NCH₃ of uncoordinated methimazole ring); 116.73, 118.98 (s, CHCH of uncoordinated methimazole ring); 117.69, 118.15 (s, CHCH of coordinated methimazole rings); 126.33, 127.15, 127.96, 133.42 (P(C₆H₅)₃); 164.37, 164.53 (s, C=S).

[RuH{κ²-N,S-mt}(PPh₃)₃], **2.** To a solution of 2-mercapto-1-methylimidazole (methimazole, 0.23 g, ca. 2 mmol) in THF (15 mL) was added LiBuⁿ (1.3 mL of a 1.6 M solution in hexanes, ca. 2.1 mmol) at room temperature. The mixture was stirred at room temperature for 5 min. Then, it was added via cannula to a slurry of [RuHCl(PPh₃)₃] (1.8 g, ca. 2 mmol) in THF (20 mL). The resulting mixture was stirred for 4 h at 60 °C. A thick yellow suspension was obtained. The yellow precipitate was filtered off. It was washed with two portions of ethanol and with one portion of petroleum ether and dried in vacuo. This product is obtained as a 1:1 mixture of diastereoisomers. No separation was attempted. The crude product can be recrystallized from dichloromethane/petroleum ether or dichloromethane/ethanol mixtures. Yield: 1.6 g, 80%. Anal. Calcd for C₅₈H₅₁N₂P₃RuS: C, 69.5; H, 5.13; N, 2.8. Found: C, 69.2; H, 5.33; N, 2.6. IR: ν(RuH) 1946 cm⁻¹. NMR data for **2** (1:1 mixture of stereoisomers): ¹H NMR (400 MHz, C₆D₆, 298 K): δ -16.00 (dt, ²J_{HP} = 27.4, ²J_{HP'} = 20.6 Hz, 1 H, RuH), 2.35 (s, 3 H, NCH₃), 5.03, 7.00 (d, ³J_{HH} = 1.3 Hz, 1 H each, CHCH); -13.65 (dt, ²J_{HP} = 27.4, ²J_{HP'} = 20.6 Hz, 1 H, RuH), 2.61 (s, 3 H, NCH₃), 5.84, 5.50 (s br, 1 H each, CHCH); 6.80–7.10, 7.49, 7.68 (m, 90 H, P(C₆H₅)₃). ³¹P{¹H} NMR (161.89 MHz, C₆D₆, 298 K): δ 48.0 (d, ²J_{PP} = 25.7 Hz), 70.4 (t, ²J_{PP} = 25.7 Hz); 48.3 (d, ²J_{PP} = 29.5 Hz), 71.8 (t, ²J_{PP} = 29.5 Hz). ¹³C{¹H} NMR (101 MHz, C₆D₆, 298 K): δ 29.99, 30.27 (NCH₃); 115.41, 115.52, 125.68, 126.12 (s, CHCH); 126.92, 127.04, 127.12, 127.89, 134.91, 135.11, 135.29, 138.36, 138.53, 138.71 (s, P(C₆H₅)₃); C=S not observed.

Catalytic Alkyne Dimerization Reactions. General procedure: A Schlenk tube was loaded with 0.02 mmol of the catalyst **1**, **2**, or **1** plus benzoic acid (5 mg, ca. 0.04 mmol) and toluene (4 mL). Then, 1 mmol of the corresponding 1-alkyne was added. The reaction mixture was heated at 85 °C using a thermostated shaking bath for 18 h. At the end of this period, the solvent was removed in vacuo. The residue was extracted with petroleum ether and filtered through a plug of silica gel. The silica gel was washed with several portions of petroleum ether, and the washings were combined with the filtrate. Removal of the solvent using a rotary evaporator first and a vacuum pump afterward afforded the corresponding alkyne dimers as a mixture of stereoisomers *Z/E/gem*. The ratios of the different stereoisomers present in the mixture were established by integration of the relevant signals in the ¹H NMR spectra.

Solution NMR Study of the Protonation Reactions of **1 and **2**.** Solutions of the respective hydride complex **1** or **2** in CD₂Cl₂ unless otherwise stated, prepared under an argon atmosphere in

NMR tubes, were frozen by immersion into liquid nitrogen. The corresponding amount of PhCOOH or HBF₄·OEt₂ (via micropipet) was added. The solvent was allowed to melt. Then, the tubes were shaken, to mix the reagents, and stored in an ethanol/liquid nitrogen bath. The samples prepared in this way were studied by NMR at low temperatures. The sample was removed from the bath and inserted into the precooled probe of the Varian UNITY-400 spectrometer at 223 K. Once shims were adjusted, the probe was warmed to the desired temperature. The NMR temperature controller was previously calibrated against a methanol sample, with the reproducibility being ±0.5 °C.

Selected Spectral Data for [Ru{κ³-H,S,S-HB(mt)₃}(H₂)(PPh₃)₂][BF₄], **3a.** ¹H NMR (400 MHz, CD₂Cl₂, 233 K): δ -8.78 (m br, 1 H, RuHB), -5.94 (br, 2 H, Ru(H₂), (T₁)_{min} = 19.8 ms), 3.38 (s, 6 H, NCH₃ of coordinated methimazole rings), 3.71 (s, 3 H, NCH₃ of uncoordinated methimazole ring), 6.249 (s br, 1 H, CHCH of uncoordinated methimazole rings; the other CHCH signals of uncoordinated methimazole ring is obscured by aromatic peaks), 6.692 (s br, 2 H, CHCH of coordinated methimazole rings; the other CHCH signal of coordinated methimazole ring is obscured by aromatic peaks), 7.22, 7.24, 7.31 (m, 30 H, P(C₆H₅)₃). ³¹P{¹H} NMR (161.89 MHz, CD₂Cl₂, 233 K): δ 43.6 (d, ²J_{PP} = 27 Hz), 45.5 (br).

Selected Spectral Data for [Ru{κ³-H,S,S-HB(mt)₃}(PPh₃)₂][BF₄], **3b.** ¹H NMR (400 MHz, CD₂Cl₂, 273 K): δ -3.62 (m br, 1 H, RuHB), 3.31 (s, 6 H, NCH₃ of coordinated methimazole rings), 3.65 (s, 3 H, NCH₃ of uncoordinated methimazole ring), 6.34, 7.51 (s br, 1 H each, CHCH of uncoordinated methimazole ring), 6.87, 7.31 (s br, 2 H each, CHCH of coordinated methimazole rings), 6.95, 7.09, 7.35 (m, 30 H, P(C₆H₅)₃). ³¹P{¹H} NMR (161.89 MHz, CD₂Cl₂, 273 K): δ 35.9 (br), 76.6 (d, ²J_{PP} = 35.9 Hz).

Selected Spectral Data for [Ru{κ²-N,S-mt}(H₂)(PPh₃)₃][BF₄], **4.** NMR data for **4** (5:1 mixture of stereoisomers): NMR data for the major isomer (relative amount 84%): ¹H NMR (400 MHz, CD₂Cl₂, 213 K): δ -10.09 (br, 2 H, Ru(H₂), (T₁)_{min} = 26.1 ms), 2.34 (s, 3 H, NCH₃), 5.29, 5.88 (s, 1 H each, CHCH); 6.40–7.80 (m, 30 H, P(C₆H₅)₃). ³¹P{¹H} NMR (161.89 MHz, CD₂Cl₂, 213 K): δ 38.7 (d, ²J_{PP} = 19.2 Hz), 48.5 (t, ²J_{PP} = 19.2 Hz). NMR data for the minor isomer (relative amount 16%): ¹H NMR (400 MHz, CD₂Cl₂, 213 K): -6.54 (br, 2 H, Ru(H₂), (T₁)_{min} = 24.6 ms), 2.43 (s, 3 H, NCH₃), 5.59, 6.03 (s br, 1 H each, CHCH); 6.40–7.80 (m, 30 H, P(C₆H₅)₃). ³¹P{¹H} NMR (161.89 MHz, CD₂Cl₂, 213 K): 37.4 (d, ²J_{PP} = 23.1 Hz), 51.3 (t, ²J_{PP} = 23.1 Hz).

X-ray Structure Determinations. Single crystals of compounds **1** and **2** were obtained and mounted on a glass fiber to carry out the crystallographic study. Crystal data and experimental details are given in Table 1. X-ray diffraction data collection was measured at 100 K on a Bruker Smart APEX CCD 3-circle diffractometer using a sealed tube source and graphite-monochromated Mo Kα radiation (λ = 0.71073 Å) at the Servicio Central de Ciencia y Tecnología de la Universidad de Cádiz. In each case four sets of frames were recorded over a hemisphere of the reciprocal space by omega scans with δ(ω) 0.30 degrees and exposure of 10 s per frame. Correction for absorption was applied by scans of equivalents using the program SADABS.²⁰ An insignificant crystal decay correction was also applied. The structure was solved by direct methods, completed by subsequent difference Fourier syntheses, and refined on F² by full matrix least-squares procedures using the programs contained in the SHELXTL package.²¹ Non-hydrogen atoms were refined with anisotropic displacement parameters. For compound **2** the ligand 2-mercapto-1-methylimidazole was found disordered. The disorder was modeled using two orientations exchanging coordination positions of nitrogen and sulfur atoms and

(20) Sheldrick, G. M. *SADABS*; University of Göttingen: Germany, 2001.

(21) Sheldrick, G. M. *SHELXTL version 6.10, Crystal Structure Analysis Package*; Bruker AXS: Madison, WI, 2000.

Table 1. Summary of Crystallographic Data for **1** and **2**

	1	2
formula	C ₅₅ H ₅₅ BN ₆ P ₂ RuS ₃	C ₅₈ H ₅₁ N ₂ P ₃ RuS
fw	1070.05	1002.05
<i>T</i> (K)	100(2)	100(2)
cryst size (mm)	0.41 × 0.27 × 0.16	0.55 × 0.39 × 0.09
cryst syst	triclinic	monoclinic
space group	<i>P</i> $\bar{1}$ (no. 2)	<i>P</i> 2 ₁ / <i>m</i> (no. 14)
cell params	<i>a</i> = 11.549(2) Å <i>b</i> = 12.335(3) Å <i>c</i> = 17.962(4) Å α = 87.68(3)° β = 82.99(3)° γ = 82.60(3)°	<i>a</i> = 11.8849(8) Å <i>b</i> = 33.952(2) Å <i>c</i> = 12.1312(9) Å β = 92.019(2)°
volume (Å ³)	2517.7(10)	4892.1(6)
<i>Z</i>	2	4
ρ_{calc} (g cm ⁻³)	1.411	1.361
μ (Mo K α) (mm ⁻¹)	0.544	0.502
<i>F</i> (000)	1108	2072
max. and min. transmn factors	0.919, 0.840	1.000, 0.829
θ range for data collection	1.67 < θ < 25.0	0.99 < θ < 25.03
reflns collected	16 622	33 651
unique reflns	8719 (<i>R</i> _{int} = 0.0282)	8597 (<i>R</i> _{int} = 0.0986)
no. of obsd reflns (<i>I</i> > 2 σ _{<i>I</i>})	7675	6734
no. of params	623	615
final <i>R</i> ₁ , <i>wR</i> ₂ values (<i>I</i> > 2 σ _{<i>I</i>})	0.0668, 0.1384	0.0506, 0.1087
final <i>R</i> ₁ , <i>wR</i> ₂ values (all data)	0.0781, 0.1925	0.0735, 0.1188
residual electron density peaks (e Å ⁻³)	+2.447, -2.184	+1.257, -0.514

the thermal parameters of involved non-hydrogen atoms constrained by EADP instructions. The site occupation factors for the two orientations refined to 0.57 and 0.43, respectively. The coordinates of hydride atoms in both cases and, for compound **1**, the hydrogen bonded to the metal and the boron of hydrotris(methimazoly)borate ligand were refined with thermal parameters linked to those of ruthenium. The remaining hydrogen atoms were geometrically positioned and isotropically refined using the riding model. The program ORTEP-3²² was used for plotting.

Results and Discussion

Preparation of the Complexes. The purple five-coordinate complex [RuHCl(PPh₃)₃] reacts cleanly with a stoichiometric amount of Na[HB(mt)₃] in MeOH at 40 °C, affording the hydride complex [Ru{ κ^3 -H,S,S-HB(mt)₃}H(PPh₃)₂] (**1**) as a yellow microcrystalline material rather than the [Ru{ κ^3 -S,S,S-HB(mt)₃}H(PPh₃)₂] isomer. This synthetic procedure is similar to the one used for the preparation of the hydrido complex [TpRuH(PPh₃)₂], modified by using Na[HB(mt)₃] instead of KTp.¹⁰ Shortly before submission of the present work, the preparation of the related bis(methimazoly)borate complex [Ru{ κ^3 -H,S,S-H₂B(mt)₂}H(PPh₃)₂] by reaction of [RuHCl(PPh₃)₃] with Na[H₂B(mt)₂] in dichloromethane was reported.⁹ Compound **1** is insoluble in MeOH, petroleum ether, or diethyl ether and very poorly soluble in acetone. Its IR spectrum (Nujol) shows a medium ν (RuH) band at 2012 cm⁻¹ and another weaker band at 2170 cm⁻¹ attributable to ν (BHRu) in the three-centered Ru—H—B bond. The values reported for ν (BHRu) in the related complexes [Ru{ κ^3 -H,S,S-HB(mt)₃}H(PPh₃)(CO)]⁸ and [Ru{ κ^3 -H,S,S-H₂B(mt)₂}H(PPh₃)₂]⁹ are 2213 and 2120 cm⁻¹, respectively. The NMR spectra of **1** are solvent dependent. Compound **1** exists in solution in the form of two diastereoisomers, **1a** and

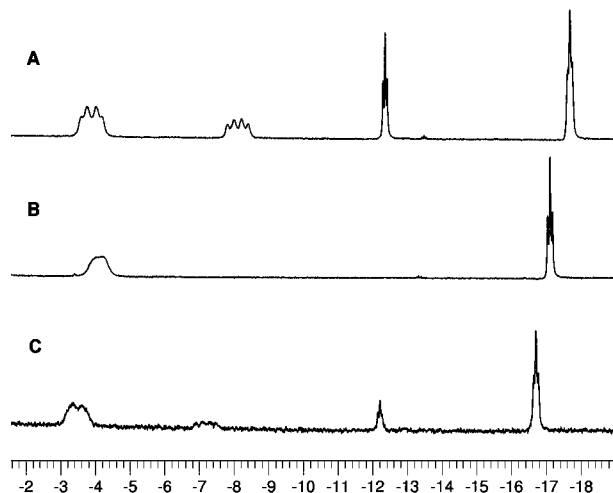


Figure 1. High-field region of the ¹H NMR spectra (400 MHz, 25 °C) of **1** in CD₂Cl₂ (A), C₂D₂Cl₄ (B), and C₆D₆ (C).

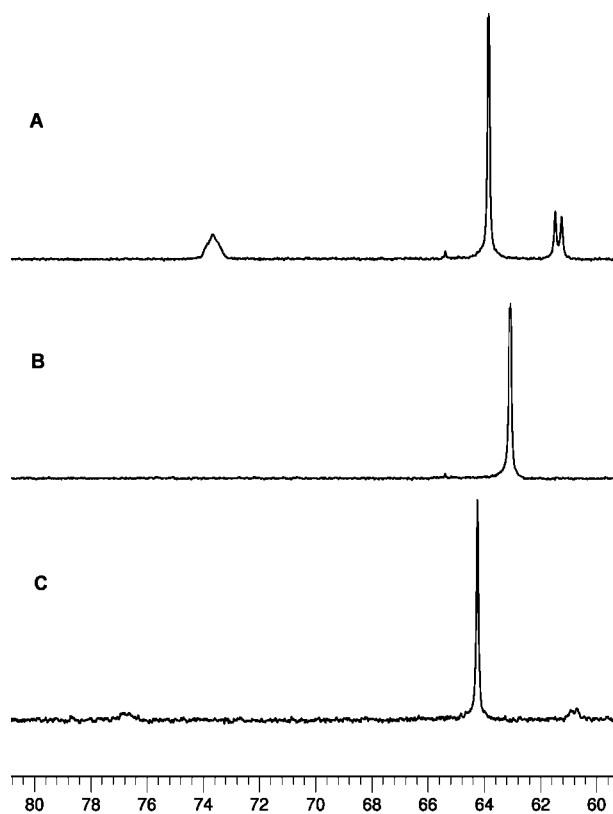


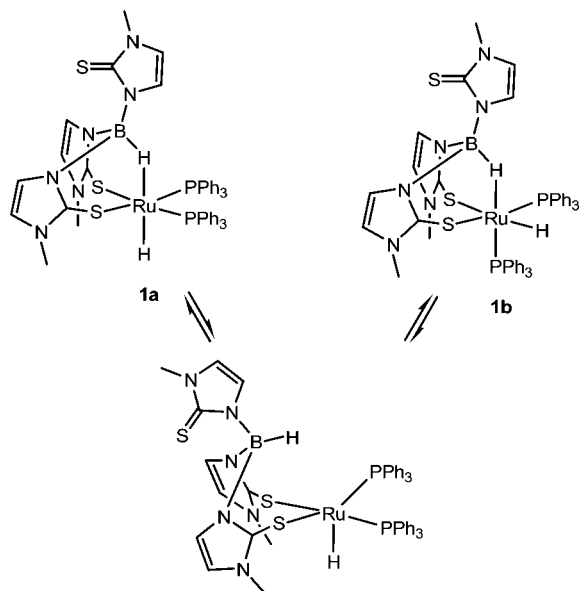
Figure 2. ³¹P{¹H} NMR spectra (161.89 MHz, 25 °C) of **1** in CD₂Cl₂ (A), C₂D₂Cl₄ (B), and C₆D₆ (C).

1b, respectively. The relative amount of each of these stereoisomers depends on the solvent used. Figures 1 and 2 show respectively the high-field region of the ¹H NMR spectra of **1** in CD₂Cl₂ (A), C₂D₂Cl₄ (B), and C₆D₆ (C) and the corresponding ³¹P{¹H} NMR spectra in the same solvents.

The ¹H NMR spectra of **1** in CD₂Cl₂ (Figure 1A) or in C₆D₆ (Figure 1C) show two sets of hydride resonances of different intensity, which appear as triplets with typical *cis*-phosphine coupling constants, along with two broad multiplet resonances ascribed to the RuHB protons of each of the stereoisomers. The intensity ratio for the two sets of resonances is 64:36 in CD₂Cl₂ and 83:17 in C₆D₆. The corresponding ³¹P{¹H} NMR spectra shown in Figures 2A and 2C show one intense singlet attributable to one of the stereoisomers (**1a**), for which

(22) Farruggia, L. J. ORTEP-3 for Windows, version 1.076. *J. Appl. Crystallogr.* **1997**, *30*, 565.

Chart 1



equivalent phosphorus atoms are expected. Along with this singlet, two resonances for the minor stereoisomer (**1b**) are observed. This is particularly evident in the spectrum in CD_2Cl_2 solution (Figure 2A), in which one of the resonances appears as one doublet and the other as a broad peak. This pattern suggests that the two phosphorus atoms are not equivalent in the stereoisomer **1b** present in minor quantity. The NMR spectra in CDCl_3 are very similar to those recorded in CD_2Cl_2 , the ratio of stereoisomers **1a**:**1b** being 77:23. At variance with this, the ^1H NMR spectrum of **1** in $\text{C}_2\text{D}_2\text{Cl}_4$ shows only one triplet hydride resonance at -17.51 ppm and one broad resonance centered at -4.50 ppm attributable to the RuHB proton (Figure 1B). In this solvent, the $^{31}\text{P}\{^1\text{H}\}$ NMR spectrum of **1** shows one singlet, indicative of the equivalence of the phosphorus atoms (Figure 2B), and both ^1H and $^{13}\text{C}\{^1\text{H}\}$ NMR spectra suggest two different chemical environments for the methimazolato rings in the ratio 2:1 as inferred from the integration of the relevant signals in the ^1H NMR spectrum. These spectral data suggest that in $\text{C}_2\text{D}_2\text{Cl}_4$ solution only the isomer **1a** is present. Hence, the structure proposed for **1a** is octahedral, with one hydride ligand and two equivalent *cis*-phosphorus atoms. This requires that the Ru–H–B interaction occurs in position *trans* to the hydride ligand, and the remaining positions are occupied by two sulfur atoms from the coordinated methimazolato rings. One of the methimazolato rings of the $\text{HB}(\text{mt})_3$ ligands remains uncoordinated. This structure is similar to that found for the complexes $[\text{Ru}\{\kappa^3\text{-H,S,S-HB}(\text{mt})_3\}\text{H}(\text{CO})(\text{PPh}_3)]$ (considering that in **1** there is one PPh_3 ligand in the position occupied by CO)⁸ and $[\text{Ru}\{\kappa^3\text{-H,S,S-H}_2\text{B}(\text{mt})_2\}\text{H}(\text{PPh}_3)_2]$.⁹ The stereoisomer **1b**, always present in minor amounts in solution, has inequivalent phosphorus atoms in a relative *cis*-disposition, as inferred from the magnitude of the $^2J_{\text{HP}}$ and $^2J_{\text{PP}}$ coupling constants. One of the phosphorus resonances appears broad, with unresolved coupling (Figure 2A), suggesting that this atom is most likely *trans* to the RuHB interaction. For this stereoisomer, the ^1H and $^{13}\text{C}\{^1\text{H}\}$ NMR spectra suggest three different chemical environments for the methimazolato rings. The structures proposed for isomers **1a** and **1b** are shown in Chart 1. The two isomers **1a** and **1b** presumably interconvert by dissociation of the BHRu interaction to yield the coordinatively unsaturated intermediate $[\text{Ru}\{\kappa^2\text{-S,S-HB}(\text{mt})_3\}\text{H}(\text{PPh}_3)_2]$, as shown in Chart 1. In this five-coordinate species, the hydride

and phosphine ligands may exchange their positions by a Berry pseudorotation-type mechanism. A similar dissociation of the BHRu linkage has been proposed to explain the observed reactivity of $[\text{Ru}\{\kappa^3\text{-H,S,S-HB}(\text{mt})_3\}\text{H}(\text{CO})(\text{PPh}_3)]$ toward phenylacetylene.⁸ However, the occurrence of a solvent-dependent equilibrium between two possible stereoisomers has not been mentioned in the case of $[\text{Ru}\{\kappa^3\text{-H,S,S-HB}(\text{mt})_3\}\text{H}(\text{CO})(\text{PPh}_3)]$ ⁸ or the recently reported $[\text{Ru}\{\kappa^3\text{-H,S,S-H}_2\text{B}(\text{mt})_2\}\text{H}(\text{PPh}_3)_2]$.⁹

The structure of the isomer **1a** was confirmed by X-ray crystal structure analysis of the solvate **1**· $\text{CH}_3\text{C}_6\text{H}_5$. An ORTEP view of the complex $[\text{Ru}\{\kappa^3\text{-H,S,S-HB}(\text{mt})_3\}\text{H}(\text{PPh}_3)_2]$ is shown in Figure 1, together with the most relevant bond distances and angles.

The structure of **1** (isomer **1a**) consists of a packing of distorted octahedral molecules of the complex and of toluene solvate molecules. As inferred spectroscopically for **1a**, the hydride and phosphine ligands are in mutually *cis* positions. There is one uncoordinated methimazolato ring pointing away from the ruthenium atom and one three-center Ru–H–B interaction in a position *trans* to the hydride ligand (H1–Ru1–H1b $159(3)^\circ$). Ru–H separations and the general dimensions compare well with the values reported for the related compounds $[\text{Ru}\{\kappa^3\text{-H,S,S-HB}(\text{mt})_3\}\text{H}(\text{CO})(\text{PPh}_3)]$ ⁸ and $[\text{Ru}\{\kappa^3\text{-H,S,S-H}_2\text{B}(\text{mt})_2\}\text{H}(\text{PPh}_3)_2]$.⁹ It is interesting to note the occurrence of short contacts between the hydride atom H1 and two *ortho* hydrogen atoms of phenyl groups of PPh_3 ligands. The separations $\text{H1}\cdots\text{H42}$ and $\text{H1}\cdots\text{H18}$ are respectively 1.96 and 2.17 Å. A short contact of 2.28 Å between the hydride atom and one *ortho* hydrogen of a phenyl group has been observed in the complex $[\text{Ru}\{\kappa^3\text{-H,S,S-HB}(\text{mt})_3\}\text{H}(\text{CO})(\text{PPh}_3)]$, indicative of a possible hydrogen-bonding interaction.⁸ In our case, the contacts are shorter and suggest stronger interactions, which contribute to fix the orientations of the PPh_3 ligands relative to the hydride ligand. This phenomenon was recognized and discussed previously by Junk and Steed for a number of hydride complexes.²³ These $\text{H}\cdots\text{H}$ interactions might account for the relatively short values of the minimum longitudinal relaxation time $(T_1)_{\text{min}}$ measured for the hydride proton in **1**. In CD_2Cl_2 solution the hydride proton in the major isomer **1a** has a $(T_1)_{\text{min}}$ of 377 ms, whereas in the minor isomer **1b** the value for $(T_1)_{\text{min}}$ of 164 ms is even shorter.

Attempts to recrystallize compound **1** from $\text{CH}_2\text{Cl}_2/\text{MeOH}$ solutions over a two-day period afforded yellow crystals of a compound other than **1**. X-ray crystal structure analysis showed it to be the methimazolato complex $[\text{RuH}\{\kappa^2\text{-N,S-mt}\}(\text{PPh}_3)_3]$ (**2**). This compound consists of a 57:43 mixture of two stereoisomers, and both stereoisomers were found present in the same crystal cell. ORTEP views of each of the stereoisomers of complex **2** are shown respectively in Figures 2 and 3, together with the most relevant bond distances and angles.

The structure of compound **2** consists of discrete distorted octahedral molecules, with a meridional disposition of the PPh_3 ligands. The methimazolato ligand appears disordered in two possible orientations with relative occupations of 57% and 43%, respectively. Each orientation corresponds to one of the two stereoisomers present in the crystal. In one of them (isomer **2a**, Figure 5) the hydride ligand appears in a position *trans* to the coordinated nitrogen, whereas the sulfur atom is *trans* to the P(2) atom. In the other isomer (**2b**, Figure 3) the hydride ligand is in a position *trans* to the sulfur atom, and the coordinated

(23) Junk, P.-C.; Steed, J. W. *J. Organomet. Chem.* **1999**, 587, 191–194.

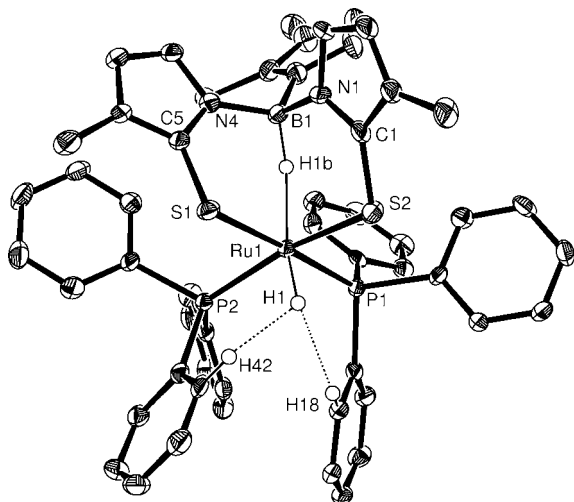


Figure 3. ORTEP drawing (50% thermal ellipsoids) of $[\text{Ru}\{\kappa^2\text{-H,S,S-HB}(\text{mt})_3\}\text{H}(\text{PPh}_3)_2]$ (**1**). Hydrogen atoms except hydride and BH have been omitted. Selected bond lengths (Å) and angles (deg) with estimated standard deviations in parentheses: Ru1–P1 2.2714(17), Ru1–P2 2.3211(16), Ru1–S2 2.3958(17), Ru1–S1 2.4570(17), Ru1–H1 1.51(7), Ru1–H1b 1.90(7), B1–H1b 1.20(7), H1···H42 1.96, H1···H18 2.17, P1–Ru1–P2 95.69(6), S1–Ru1–S2 88.88(6), P1–Ru1–S2 89.65(6), P2–Ru1–S1 84.54(6), N4–B1–N1 105.5(5), H1–Ru1–H1b 159(3); B1–H1b–Ru1 141.46(5).

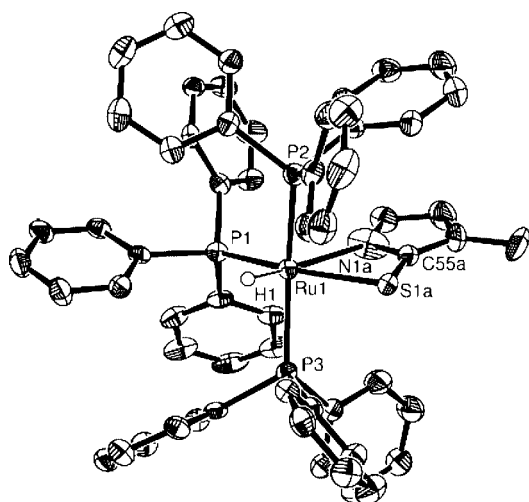


Figure 4. ORTEP drawing (50% thermal ellipsoids) of the isomer **2a** (57%) of $[\text{RuH}\{\kappa^2\text{-N,S-mt}\}(\text{PPh}_3)_3]$ (**2**). Hydrogen atoms except hydride have been omitted. Selected bond lengths (Å) and angles (deg) with estimated standard deviations in parentheses: Ru–N(1A) 2.240(14), Ru–S(1A) 2.480(3), Ru–H(1) 1.55(4), Ru–P(1) 2.2686(11), Ru–P(2) 2.3454(11), Ru–P(3) 2.3493(10), C(55A)–S(1A) 1.661(14), C(55A)–N(1A) 1.191(16), P(2)–Ru–P(3) 155.68(4), P(2)–Ru–P(1) 100.15(4), P(3)–Ru–P(1) 98.10(4), P(1)–Ru–H(1) 98.0(14), P(1)–Ru–S(1A) 164.63(13), N(1A)–Ru–H(1) 155.3(14), N(1A)–Ru–S(1A) 61.1(4), N(1A)–C(55A)–S(1A) 114.0(11).

nitrogen atom is *trans* to P(2). All bond lengths and angles in both stereoisomers **2a/b** are identical except those affecting directly the atoms of the methimazolate ring. The hydride ligand was located in a difference Fourier map and refined, leading to a Ru–H separation of 1.55(4) Å. The Ru–N and Ru–S bond lengths as well as the dimensions of the methimazolate ligand

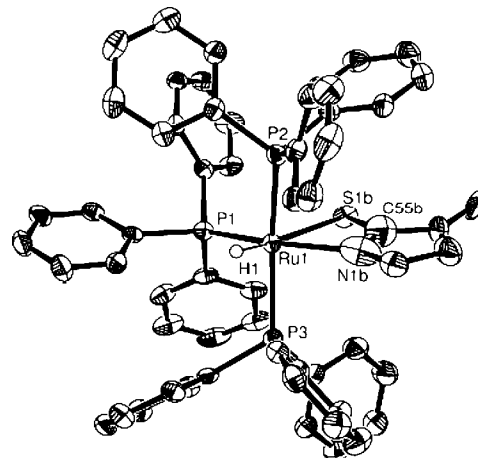


Figure 5. ORTEP drawing (50% thermal ellipsoids) of the isomer **2b** (43%) of $[\text{RuH}\{\kappa^2\text{-N,S-mt}\}(\text{PPh}_3)_3]$ (**2**). Hydrogen atoms except hydride have been omitted. Selected bond lengths (Å) and angles (deg) with estimated standard deviations in parentheses: Ru–N(1B) 2.28(2), Ru–S(1B) 2.586(5), C(55B)–S(1B) 1.777(15), C(55B)–N(1B) 1.21(3), P(1)–Ru–S(1B) 161.6(6), N(1B)–Ru–H(1) 100.4(15), N(1B)–Ru–S(1B) 66.2(6), N(1B)–C(55B)–S(1B) 125.5(19). All the other bond distances and angles are identical to those in **2a**.

compare well with the values reported in the literature for ruthenium methimazolates, such as $[\text{Ru}\{\kappa^2\text{-N,S-mt}\}_2\text{-(PPh}_3)_2]$ ²⁴ or $[\text{Ru}\{\kappa^2\text{-N,S-mt}\}(\text{R})(\text{CO})(\text{PPh}_3)_2]$ (R = CH=CHC₆H₄Me, CPh=CHPh, CH=CHC₆H₉, C₆H₅; C≡CC₆H₅).²⁵

These results suggest that the HB(mt)₃ ligand in **1** undergoes a slow degradation process in CH₂Cl₂/MeOH solution with involves cleavage of the B–N bond of at least one of the methimazolates rings, leading to **2a/b** as the only identified isolable products, with yields close to 50% based upon the initial amount of ruthenium complex. The cleavage of methimazolyl groups from either Na[H₂B(mt)₂] or Na[HB(mt)₃] to furnish methimazolates complexes has precedents in the recent literature.^{24,26} Complex **2** can be more adequately prepared in high yield by reaction of $[\text{RuHCl}(\text{PPh}_3)_3]$ with Li(mt) in THF. In this fashion a mixture of stereoisomers was also obtained. Isomer separation was not attempted. The ¹H, ³¹P{¹H}, and ¹³C{¹H} NMR spectra of **2** in C₆D₆ solution are consistent with the presence of two stereoisomers in a 55:45 ratio (by integration of the relevant hydride resonances in the ¹H NMR spectrum). Thus, two separate high-field hydride resonances (doublet of triplets, X part of an AM₂X spin system) are observed in the ¹H NMR spectrum, whereas the ³¹P{¹H} NMR spectrum shows two sets of phosphorus resonances, which are consistent with the presence of two separate A₂M spin systems as expected.

Catalytic Dimerization of 1-Alkynes. The catalytic dimerization of 1-alkynes is atom-economical and a straightforward method for the preparation of conjugated enynes, which are important building blocks in organic synthesis.^{27–31} Complexes **1** and **2** are catalyst precursors for the dimerization of 1-alkynes to give the corresponding enynes as mixtures of *Z*, *E*, and in some instances also *gem*-stereoisomers. The reactions were carried out in toluene at 85 °C for a period

(26) Hill, A. F.; Smith, M. K. *Dalton Trans.* **2006**, 28–30.

(24) Dewhurst, R. D.; Hansen, A. R.; Hill, A. F.; Smith, M. K. *Organometallics* **2006**, *25*, 5843–5846.

(25) Wilton-Ely, J. D. E. T.; Honarkah, S. J.; Wang, M.; Tocher, D. A.; Slawin, A. M. Z. *Dalton Trans.* **2005**, 1930–1939.

(27) (a) Trost, B. M.; Chan, C.; Ruhter, G. *J. Am. Chem. Soc.* **1987**, *109*, 3486–3487. (b) Ohshita, J.; Furumori, K.; Matsuguchi, A.; Ishikawa, M. *J. Org. Chem.* **1990**, *55*, 3277–3280. (c) Horton, A. D. *J. Chem. Soc., Chem. Commun.* **1992**, 185–187. (d) Barluenga, J.; González, J. M.; Llorente, I.; Campos, P. *J. Angew. Chem., Int. Ed. Engl.* **1993**, *32*, 893–894. (e) Straub, T.; Haskel, A.; Eisen, M. S. *J. Am. Chem. Soc.* **1995**, *117*, 6364–6365.

Table 2. Product Distribution for Alkyne Dimerization Reactions Catalyzed by Compounds **1** and **2**^a

Entry	Catalyst	Substrate	Yield (%)	Isomer distribution (%)		
				(E)	(Z)	gem
1	1	PhC≡CH	91	47	53	-
2	1	Me ₃ SiC≡CH	65	11	80	9
3	1	BrC ₆ H ₄ C≡CH	59	50	50	-
4	1	CH ₃ C ₆ H ₄ C≡CH	98	64	36	-
5	1	CF ₃ C ₆ H ₄ C≡CH	95	81	19	-
6	2	PhC≡CH	72	33	55	12
7	2	BrC ₆ H ₄ C≡CH	45	14	74	12
8	2	CH ₃ C ₆ H ₄ C≡CH	93	23	67	10
9	2	CF ₃ C ₆ H ₄ C≡CH	60	26	63	11

^a Reaction conditions: toluene, 85 °C, 18–20 h, 2% catalyst.

of 18–20 h with catalyst loads of 2%. The enynes were isolated at the end of the reaction period upon solvent removal, extraction with petroleum ether, and flash chromatography on silica gel. The yields of isolated enynes and the stereoisomer composition of the mixtures for each of the catalytic runs are shown in Table 2.

The yields of isolated enynes were in the range 45–98%. When **2** was used as catalyst precursor, mixtures of *Z*, *E*, and *gem*-stereoisomers were obtained in all cases. The only instance in which a *gem*-stereoisomer was observed when **1** was used

as catalyst was the reaction of Me₃SiC≡CH. The *Z/E* stereoisomer ratio was dependent on the R group in the alkyne. We were interested in testing the ability of **1** and **2** to act as catalyst precursors for the addition of benzoic acid to 1-alkynes to yield the corresponding enol esters. Thus, a catalytic reaction test was conducted with benzoic acid and phenylacetylene (2:1 ratio) using a 2% load of **1** in toluene at 85 °C. No enol ester resulted from this test. Instead, the corresponding enyne was recovered quantitatively. However, the *Z/E* stereoisomer ratio 88:12 was very different from the value of 53:47 for the *Z/E* ratio obtained in the direct dimerization run (i.e., with no added PhCOOH). The effect was not so marked in the reaction catalyzed by **2**. In this case the *Z/E* stereoisomer ratio changed from 55:33 to 76:10 in the presence of PhCOOH, with a content of *gem*-isomer that remained essentially unaltered. Clearly, the addition of PhCOOH has an effect on these catalytic systems, modifying the stereoselectivity. Thus we carried out a series of dimerization reactions with a 2% catalyst load and catalytic amount (4–5%) of PhCOOH. Results are summarized in Table 3.

Figure 6 shows a bar diagram that allows a direct comparison of the differences in percentages of *Z* stereoisomer in the enyne mixtures for the reactions catalyzed by **1** and **1**+PhCOOH, respectively.

A very significant increase in the relative amounts of the *Z* stereoisomers is produced in all cases. The addition of PhCOOH not only induces a significant change in the stereoselectivity of these reactions but also modifies the catalytic reaction rate and hence the turnover frequency (TOF = (moles of converted alkyne)/[(moles of catalyst)(time)]). We monitored by ¹H NMR in toluene-*d*₈ at 85 °C the catalytic conversion of phenylacetylene into the corresponding enynes by following the disappearance of the acetylenic proton resonance of phenylacetylene at ca. 3 ppm. The resulting plot is shown in Figure 7.

The dimerization reaction catalyzed by **1** is very fast and reaches quantitative conversion within the initial 5 min (TOF

(28) (a) Bianchini, C.; Peruzzini, M.; Zanobini, F.; Frediani, P.; Albinati, A. *J. Am. Chem. Soc.* **1991**, *113*, 5453–5454. (b) Bianchini, C.; Innocenti, P.; Peruzzini, M.; Romerosa, A.; Zanobini, F.; Frediani, P. *Organometallics* **1996**, *15*, 272–285. (c) Duchateau, R.; van Wee, C. T.; Meetsma, A.; Teuben, J. H. *J. Am. Chem. Soc.* **1993**, *115*, 4931–4932. (d) Jun, C.-H.; Lu, Z.; Crabtree, R. H. *Tetrahedron Lett.* **1992**, *33*, 7119–7120. (e) Matsuzaka, H.; Takagi, Y.; Ishii, Y.; Nishio, M.; Hidai, M. *Organometallics* **1995**, *14*, 2153–2155.

(29) (a) Bianchini, C.; Frediani, P.; Masi, D.; Peruzzini, M.; Zanobini, F. *Organometallics* **1994**, *13*, 4616–4632. (b) Slugovc, C.; Mereiter, K.; Zobetz, E.; Schmid, R.; Kirchner, K. *Organometallics* **1996**, *15*, 5275–5277. (c) Katayama, H.; Nakayama, M.; Nakano, T.; Wada, C.; Akamatsu, K.; Ozawa, F. *Macromolecules* **2004**, *37*, 13–17. (d) Wakatsuki, Y.; Yamazaki, H.; Kumegawa, N.; Satoh, T.; Satoh, Y. *J. Am. Chem. Soc.* **1991**, *113*, 9604–9610. (e) Wakatsuki, Y.; Koga, N.; Yamazaki, H.; Morokuma, K. *J. Am. Chem. Soc.* **1994**, *116*, 8105–8111. (f) Echavarren, A. M.; López, J.; Santos, A.; Montoya, J. *J. Organomet. Chem.* **1991**, *414*, 393–400. (g) Trost, B. M.; Dean Toste, F. D.; Pinkerton, A. B. *Chem. Rev.* **2001**, *101*, 2067–2096. (h) Le Paih, J.; Monnier, F.; Derien, S.; Dixneuf, P. H.; Clot, E.; Eisenstein, O. *J. Am. Chem. Soc.* **2003**, *125*, 11964–11975. (i) Naota, T.; Takaya, H.; Murahashi, S.-I. *Chem. Rev.* **1998**, *98*, 2599–2660.

(30) (a) Daniels, M.; Kirss, R. U. *J. Organomet. Chem.* **2007**, *692*, 1716–1725. (b) Bruce, M. I.; Hall, B. C.; Zaitseva, N. N.; Skelton, B. W.; White, A. H. *J. Organomet. Chem.* **1996**, *522*, 307–310. (c) Yang, S.-M.; Chan, C.-W.; Cheung, K.-K.; Che, C.-M.; Peng, S.-M. *Organometallics* **1997**, *16*, 2819–2826. (d) Albertin, G.; Antonietti, S.; Bordignon, E.; Cazzaro, F.; Ianelli, S.; Pelizzi, G. *Organometallics* **1995**, *14*, 4114–4125.

(31) (a) Yi, Ch. S.; Liu, N.; Rheingold, A. L.; Liable-Sands, L. M.; Guzei, I. A. *Organometallics* **1997**, *16*, 3729–3731. (b) Yi, Ch. S.; Liu, N. *Organometallics* **1998**, *17*, 3158–3160. (c) Yi, Ch. S.; Liu, N. *Organometallics* **1996**, *15*, 3968–3971.

Table 3. Product Distribution for Alkyne Dimerization Reactions Catalyzed by Compounds **1** and **2** in the Presence of Catalytic Amounts of PhCOOH^a

Entry	Catalyst	Substrate	Yield (%)	Isomer distribution (%)		
				(E)	(Z)	gem
1	1	PhC≡CH	100	12	88	-
2	1	BrC ₆ H ₄ C≡CH	37	13	87	-
3	1	CH ₃ C ₆ H ₄ C≡CH	86	14	86	-
4	1	CF ₃ C ₆ H ₄ C≡CH	84	25	75	-
5	2	PhC≡CH	79	10	76	14

^a Reaction conditions: toluene, 85 °C, 18–20 h, 2% catalyst, 4–5% PhCOOH.

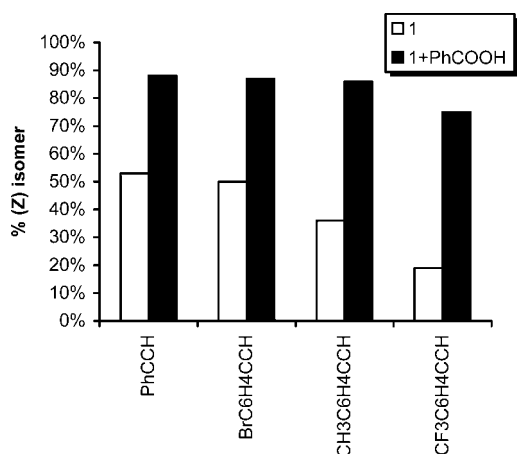


Figure 6. Differences in percentages of Z stereoisomer in the enyne mixtures for the reactions catalyzed by **1** (white bars) and **1**+PhCOOH (black bars).

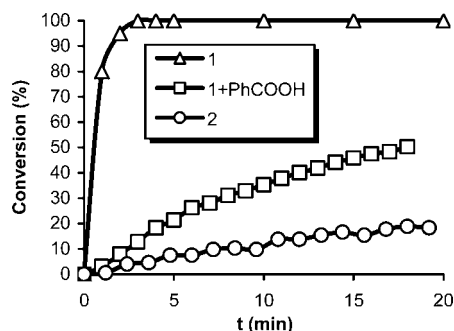


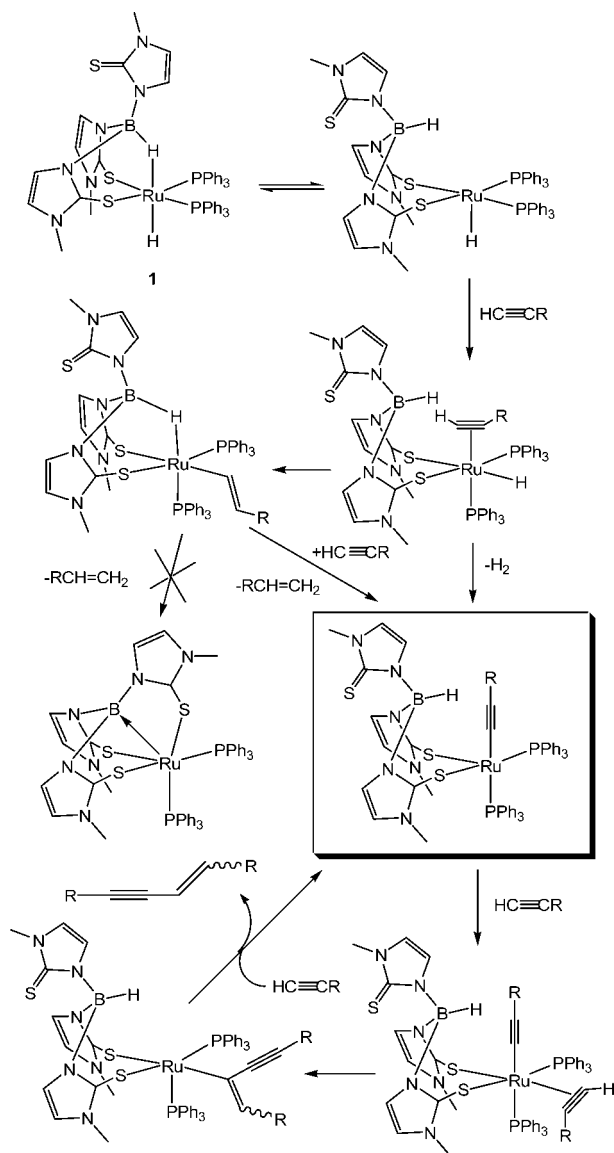
Figure 7. Plot of conversion as a function of time for the dimerization reaction of phenylacetylene in toluene-*d*₈ catalyzed by **1** (Δ), **1**+PhCOOH (□), or **2** (○) at 85 °C. Catalyst load 2% (PhCOOH 4%).

600 h⁻¹). In the presence of benzoic acid, the profile of the conversion versus time curve changes, and the reaction rate is slower. At 20 min the conversion is ca. 50% (TOF 92 h⁻¹). At this time, the dimerization reaction catalyzed by **2** has a conversion below 20% (TOF 31 h⁻¹), suggesting that compound **2** is a much less active catalyst than **1** or even **1**+PhCOOH.

Therefore, the increase in stereoselectivity observed for the reactions carried out with added PhCOOH simultaneously involves a decrease in the activity of the catalyst. This suggests that the nature of the catalytically active species is modified to a great extent when the reactions are carried out with **1** as catalyst precursor either in the absence or in the presence of benzoic acid. We carried out stoichiometric reactions of **1** with 2 equiv of PhCOOH in toluene at 85 °C in an attempt to understand the true nature of the modified complex. It is reasonable to consider the formation of [Ru(κ³-H,S,S-HB(mt)₃)(PhCOO)(PPh₃)] under these conditions. An orange solid was isolated from this reaction. The resulting material showed IR bands attributable to coordinated benzoate, but no bands for RuH or BH bands were present. However, the ¹H and ³¹P{¹H} NMR spectra of this substance indicated that it is actually a complex mixture of products (multiple phosphorus resonances in the ³¹P{¹H} NMR spectrum, including free PPh₃) from which no conclusions could be drawn. Monitoring of the reaction of **1** with 2 equiv of PhCOOH in C₆D₆ at room temperature showed the slow formation of free PPh₃ and the concomitant appearance of one singlet resonance at 31.47 ppm corresponding to an unidentified species. When the temperature was raised above 50 °C, many new phosphorus resonances appeared, and the only peak that could be recognized was the one corresponding to free PPh₃.

The dimerization of 1-alkynes to enynes is known to occur via either alkynyl–vinylidene or alkynyl–alkyne coupling.^{15,28–31} We can propose a mechanism for the catalytic dimerization of 1-alkynes mediated by **1** as shown in Scheme 1.

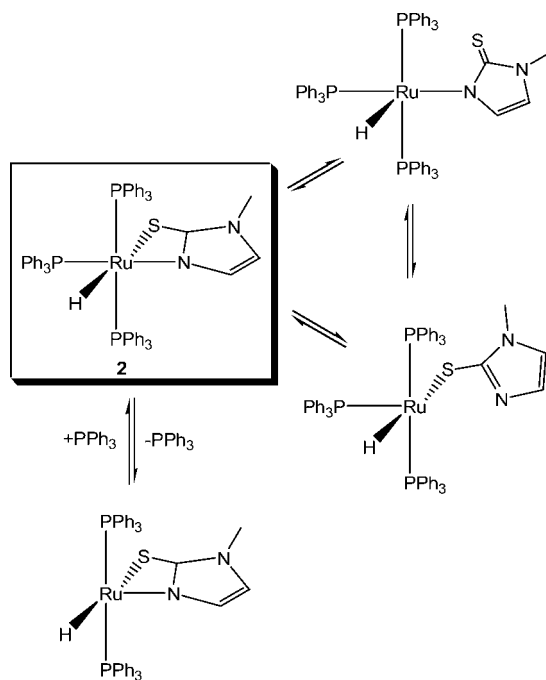
As it has been proposed by Hill and co-workers for [Ru{κ³-H,S,S-HB(mt)₃}H(CO)(PPh₃)], the dissociation of the BHRu linkage provides a vacant coordination site for the phenylacetylene.⁸ This is followed by hydroteneation to provide the intermediate [Ru{κ³-H,S,S-HB(mt)₃}(CH=CHPh)(CO)(PPh₃)], which undergoes BH activation and styrene reductive elimination, furnishing the ruthenaboratrane complex [Ru(κ³-S,S,S-B(mt)₃)(CO)(PPh₃)] as the final product. In our case, the catalytic cycle starts in a similar fashion, but the corresponding ruthenaboratrane [Ru{κ³-S,S,S-B(mt)₃}(PPh₃)₂] has never been observed in our system. The catalytically active species is most likely a coordinatively unsaturated alkynyl complex of the type [Ru{κ²-S,S-HB(mt)₃}(C≡CR)(PPh₃)₂], as it has been postulated

Scheme 1. Proposed Reaction Sequence for the Catalytic Dimerization of 1-Alkynes Mediated by Compound 1


in other instances for the ruthenium-mediated dimerization of 1-alkynes.^{15,29–31} This species might be generated directly from the π -alkyne intermediate upon H₂ elimination, or alternatively from the vinyl species [Ru(κ^3 -H,S,S-HB(mt)₃)(CH=CHR)(PPh₃)₂] upon reaction with one alkyne molecule and release of styrene. Coordination of another alkyne molecule to the alkynyl intermediate is followed by alkyne–alkynyl coupling. The reaction with further alkyne releases the final enynyl product and regenerates the catalytically active alkynyl complex.

The catalytic cycle shown in Scheme 1 can be adapted to account for the 1-alkyne dimerization reactions catalyzed by compound 2. In this case, the initial step would be a phosphine dissociation to provide a vacant coordination site. However, this vacant site might be also generated considering a hemilabile behavior for the methimazolite ligand, changing its coordination from κ^2 -N,S to either κ^1 -N or κ^1 -S, as shown in Scheme 2.

In each case, the reaction with 1-alkyne followed by elimination of either hydrogen or styrene would lead to a coordinatively unsaturated σ -alkynyl complex, which might act as the catalytically active species. The fact that several pathways are feasible accounts for the low stereoselectivity observed in the enynes, resulting from the reactions using 2 as catalyst precursor.

Scheme 2


The 1-alkyne dimerization reactions mediated by 1 in the presence of PhCOOH seem to follow a different pathway, which involves the modification of the catalyst precursor. For this reason, we carried out further spectroscopic studies of the interaction of 1 with benzoic acid in an attempt to identify the chemical changes in the structure of the catalyst precursors. The effect of a stronger acid such as HBF₄ was also studied.

Protonation Reactions. The reaction of 1 with PhCOOH in the complex to acid ratio of 1:2 in CD₂Cl₂ was monitored in the temperature range –60 to +25 °C. The VT ¹H and ³¹P{¹H} NMR spectra of the mixture are shown in Figure 8.

Apparently, no significant changes were observed in the hydride region of the ¹H NMR spectrum or in the ³¹P(¹H) NMR

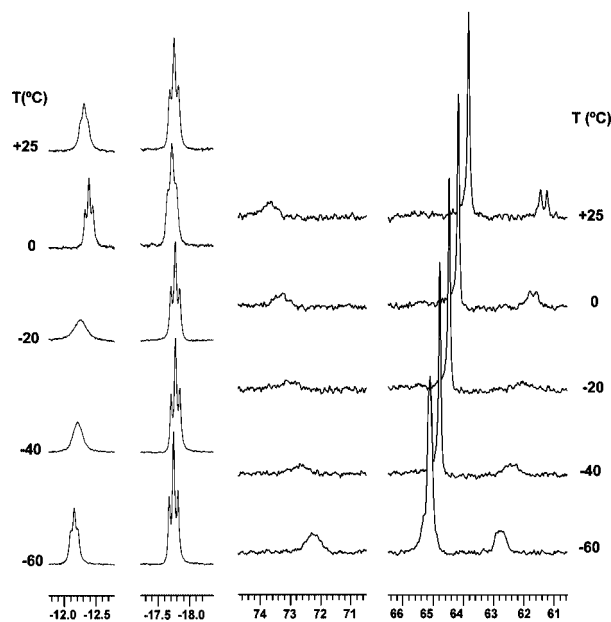


Figure 8. VT ¹H NMR (left, hydride region, 400 MHz) and VT ³¹P{¹H} NMR (right, 161.89 MHz) of a sample made up by addition of 2 equiv of PhCOOH to a CD₂Cl₂ solution of 1 at –80 °C, followed by subsequent warming to the indicated temperatures.

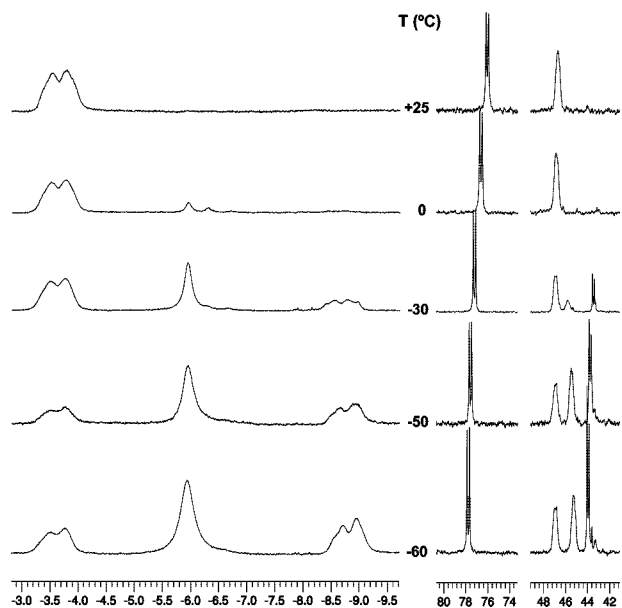


Figure 9. VT ^1H NMR (left, hydride region, 400 MHz) and VT $^{31}\text{P}\{^1\text{H}\}$ NMR (right, 161.89 MHz) of a sample made up by addition of an excess of $\text{HBF}_4 \cdot \text{OEt}_2$ to a CD_2Cl_2 solution of **1** at -80°C followed by subsequent warming to the indicated temperatures.

spectrum, apart from a broadening of the hydride resonance at -12.15 ppm attributed to isomer **1b**. The longitudinal relaxation time T_1 measured for this resonance at -60°C was 23 ms. This is considerably shorter than the value of 164 ms for the T_1 of the hydride resonance of **1b** measured in the absence of PhCOOH at the same temperature. On the other hand, the value of T_1 for the resonance at -17.74 ppm is 454 ms, being very similar to the T_1 of 490 ms measured for the hydride resonance of **1a** in the absence of PhCOOH at -60°C . As the temperature rises, the T_1 of the hydride resonance at ca. -12.2 ppm gets gradually shorter, reaching a minimum value, $(T_1)_{\text{min}}$, of 5.9 ms at -20°C . The value of $(T_1)_{\text{min}}$ for the resonance at ca. -17.7 ppm is 384 ms at $+25^\circ\text{C}$, a value very similar to that found for the hydride resonance of **1a** in the absence of PhCOOH (356 ms at $+25^\circ\text{C}$). The resonances of the proton of the RuHB fragment for each of the species are present in the entire range of temperature, suggesting that the RuHB linkage is not affected by the presence of PhCOOH . These observations suggest that only the isomer **1b** interacts to a great extent with PhCOOH . Under these conditions, the formation of a species containing a dihydrogen bond, namely, $[\text{Ru}\{\kappa^3\text{-H,S,S-HB}(\text{mt})_3\}(\text{H}\cdots\text{HOOC-Ph})(\text{PPh}_3)_2]$, should be expected. A shortening of the T_1 for the hydride resonance with respect to the value of the parent hydride complex is a characteristic of dihydrogen-bonded complexes,³² as it is also a minimum shift in the position hydride resonance and the fact that the $^{31}\text{P}\{^1\text{H}\}$ NMR remains essentially unchanged. However, the observed $(T_1)_{\text{min}}$ of 5.9 ms is very short even considering the formation of a cationic dihydrogen complex of the type $[\text{Ru}\{\kappa^3\text{-H,S,S-HB}(\text{mt})_3\}(\text{H}_2)(\text{PPh}_3)_2]^+$, for a which a $(T_1)_{\text{min}}$ in the range 15 to 30 ms should be expected. In order to explore the possibility of the formation of an intermediate dihydrogen complex in the system, we carried out the protonation with an excess of $\text{HBF}_4 \cdot \text{OEt}_2$ in CD_2Cl_2 . The VT ^1H and $^{31}\text{P}\{^1\text{H}\}$ NMR spectra of the mixture are shown in Figure 9.

Upon addition of an excess of $\text{HBF}_4 \cdot \text{OEt}_2$ at -80°C , both the ^1H and $^{31}\text{P}\{^1\text{H}\}$ NMR spectra are completely different from those of the parent hydride complex **1**. At -60°C , the ^1H NMR spectrum shows in the hydride region two broad multiplet resonances ascribed to RuHB protons, plus one broad resonance centered at -5.95 ppm, for which the shortest T_1 measured was 19.8 ms at -30°C . The shortest T_1 for the broad RuHB resonances is 111 ms for the signal at -8.6 ppm and 136 ms for the signal -3.6 ppm. The $^{31}\text{P}\{^1\text{H}\}$ NMR spectrum at -60°C shows two sets of resonances corresponding to two AM spin systems. Each of the sets consists of one doublet and one broad resonance with unresolved coupling. As the temperature rises, the intensity of one of the sets increases, whereas the other one decreases. In analogous fashion, in the ^1H NMR spectra the broad signal at -5.95 ppm and the RuHB resonance at -8.6 ppm decrease as the temperature is raised. At 25°C , only one species is observed, having inequivalent phosphorus atoms and maintaining the RuHB interaction. These observations are consistent with the formation of a metastable cationic dihydrogen complex $[\text{Ru}\{\kappa^3\text{-H,S,S-HB}(\text{mt})_3\}(\text{H}_2)(\text{PPh}_3)_2]^+$ (**3a**) at low temperature, having inequivalent phosphorus atoms as inferred from the $^{31}\text{P}\{^1\text{H}\}$ NMR spectra. We have observed no spectral evidence for the protonation at a site other than the hydride, i.e., the kinetic S-protonation of the pendant methimazolyl group. If this indeed happens, the proton is rapidly transferred to the hydride site, furnishing the dihydrogen complex **3a**. As temperature rises, the dihydrogen ligand is lost and a new species having also inequivalent phosphorus atoms and an intact RuHB interaction is generated. This species has an intense green color, and it is already present at -60°C . Attempts to isolate this compound as a solid were unsuccessful. The fact that the protonation experiments were performed under an argon atmosphere rules out the formation of a dinitrogen complex by substitution of the coordinated dihydrogen molecule. The spectral data are consistent with the presence of a coordinatively unsaturated complex of the type $[\text{Ru}\{\kappa^3\text{-H,S,S-HB}(\text{mt})_3\}(\text{PPh}_3)_2]^+$ (**3b**), generated upon dihydrogen loss, as shown in Scheme 3, although the formation of a 18-electron complex with a coordinated $[\text{BF}_4]^-$ anion cannot be ruled out.

Although this assignment must be regarded as tentative, it is consistent with spectral data and it is also reasonable from the chemical point of view. There are many examples in the literature of labile dihydrogen complexes that furnish 16-electron species upon release of the coordinated H_2 molecule. In some instances the resulting coordinatively unsaturated species have been isolated and characterized in full.^{19,33} Summing up, the protonation reaction of **1** with HBF_4 leads to the formation of the metastable cationic dihydrogen complex **3a**, which upon H_2 loss generates either the 16-electron complex **3b** or its labile adduct with $[\text{BF}_4]^-$. These results are completely different from those obtained in the reaction of **1** with PhCOOH . Hence, the resonance having the very short $(T_1)_{\text{min}}$ of 5.9 ms in the ^1H NMR spectrum cannot be attributed to the formation of the dihydrogen complex **3a**, for which the shortest T_1 measured was 19.8 ms. Furthermore, the value of 5.9 ms for $(T_1)_{\text{min}}$ would imply an unrealistically short H–H bond distance, shorter than 0.74 \AA .³⁴ Our research group^{17,35} and other researchers^{36,37} have recently

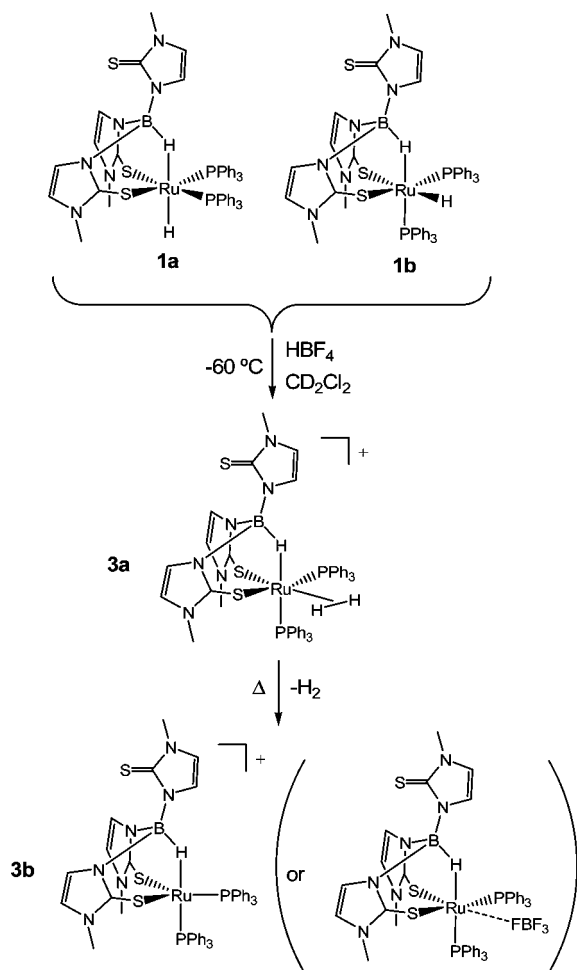
(32) (a) Custelcean, R.; Jackson, J. S. *Chem. Rev.* **2001**, *101*, 1963–1980. (b) Epstein, L. M.; Belkova, N. V.; Shubina, E. S. In *Recent Advances in Hydride Chemistry*; Peruzzini, M., Poli, R. Eds.; Elsevier: Amsterdam, The Netherlands, 2001; Chapter 14, pp 391–418, and references therein.

(33) (a) de los Ríos, I.; Jiménez-Tenorio, M.; Puerta, M. C.; Salcedo, I.; Valerga, P. *J. Chem. Soc., Dalton Trans.* **1997**, 4619–4624. (b) Barthazy, P.; Stoop, R. M.; Wörle, M.; Togni, A.; Mezzetti, A. *Organometallics* **2000**, *19*, 2844–2852. (c) Chin, B.; Lough, A. J.; Morris, R. H.; Schweitzer, C. T.; D'Agostino, C. *Inorg. Chem.* **1994**, *33*, 6278–6288.

(34) Morris, R. H. *Coord. Chem. Rev.* **2008**, *252*, 2381–2394.

(35) Jiménez-Tenorio, M.; Palacios, M. D.; Puerta, M. C.; Valerga, P. *Inorg. Chem.* **2007**, *46*, 1001–1012.

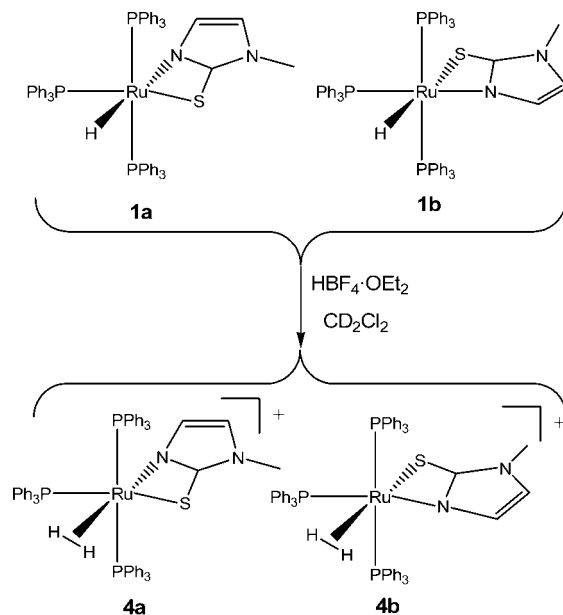
Scheme 3



reported several examples of hydride-proton transfer reactions for which very short T_1 values have been measured, in some cases shorter than 1 ms. Although the presence of paramagnetic impurities undergoing degenerate spin exchange with the parent hydride complex has been invoked to justify such observations in certain instances,³⁷ there is actually no satisfactory explanation for the anomalous shortening of T_1 . Although everything seems to point to the formation of a dihydrogen-bonded species between **1** and PhCOOH , this represents another example of a system having an ultrafast hydridic proton relaxation. The reasons why this occurs remain as yet unknown. It is important to remark on the fact that only the isomer **1b** seems to interact with PhCOOH , whereas the isomer **1a** is not visibly affected. Clearly, the protonation reactions of **1** are not simple processes, as recently remarked by Lledós and co-workers referring in general to the protonation of transition metal hydrides.³⁸ The different behavior of isomers **1a** and **1b** toward PhCOOH might be related to the observed increase in the stereoselectivity of the dimerization of 1-alkynes catalyzed by **1** in the presence of PhCOOH , although at this stage it is not possible to rationalize the exact cause for this fact.

We also studied the protonation reaction of the hydridomethimazolato complex **2** using HBF_4 in CD_2Cl_2 . Since compound

2 exists in solution as a 55:45 mixture of two diastereoisomers **1a** and **1b**, the protonation reaction leads to two isomeric cationic dihydrogen complexes $[\text{Ru}(\text{mt})(\text{H}_2)(\text{PPh}_3)_3][\text{BF}_4]$ (**4a** and **4b**), as shown.



The resulting mixture of dihydrogen complexes **4a/4b** is not equimolar. An isomer ratio of ca. 5:1 was observed. This allowed the accurate determination of the NMR resonances due to each of the isomers. However, the spectral data do not tell unambiguously which of the isomers, **4a** or **4b**, is respectively the major and the minor species in the mixture. For each of the dihydrogen complexes, the ^1H NMR spectra show one broad high-field resonance corresponding to the coordinated H_2 . These resonances exhibit $(T_1)_{\text{min}}$ values of 24.6 ms (minor stereoisomer) and 26.1 ms (major stereoisomer), respectively, fully consistent with the formulation of **4a** and **4b** as dihydrogen complexes. The $^{31}\text{P}\{^1\text{H}\}$ NMR spectra of **4a/4b** consist of two sets of resonances in the approximate ratio 5:1, corresponding to A_2M spin systems, indicative of the *mer*-disposition of the PPh_3 ligands in these derivatives, as in the parent complex **2**. The dihydrogen complexes **4a/4b** decompose to a mixture of uncharacterized species when the temperature is raised above $0\text{ }^\circ\text{C}$.

Conclusions

The hydrotris(methimazolyl)borate complex $[\text{Ru}\{\kappa^3\text{-H,S,S-HB}(\text{mt})_3\}\text{H}(\text{PPh}_3)_2]$ (**1**) was prepared and characterized. **1** exists in solution as a mixture of two stereoisomers, namely, **1a** and **1b**, in proportions that are solvent-dependent. The reaction with $\text{CH}_2\text{Cl}_2/\text{MeOH}$ leads to the hydridomethimazolato complex $[\text{RuH}\{\kappa^2\text{-N,S-mt}\}(\text{PPh}_3)_3]$ (**2**), which exists both in solution and in the solid state as a mixture of stereoisomers **2a/2b**. Both **1** and **2** are catalysts for the dimerization of 1-alkynes to the corresponding enynes, which are obtained as mixtures of stereoisomers. The addition of PhCOOH to **1** produces an increase in the stereoselectivity of the catalytic dimerization reaction, directing the reaction toward the formation of the *Z*-stereoisomers. A NMR study of the interaction of **1** with PhCOOH in CD_2Cl_2 has revealed the formation of what appears to be a dihydrogen-bonded complex between isomer **1b** and PhCOOH , but the resulting species exhibits an anomalously short $(T_1)_{\text{min}}$ of 5.9 ms, for which no satisfactory explanation

(36) Castellanos, A.; Ayllón, J. A.; Sabo-Etienne, S.; Donnadieu, B.; Chaudret, B.; Yao, W.; Kavallieratos, K.; Crabtree, R. H. *C. R. Acad. Sci. Paris, Ser. IIC* **1999**, *2*, 359–368.

(37) Belkova, N. V.; Collange, E.; Dub, P.; Epstein, L. M.; Lemenovskii, D. A.; Lledós, A.; Maresca, O.; Maseras, F.; Poli, R.; Revín, P. O.; Shubina, E. S.; Vorontsov, E. V. *Chem.—Eur. J.* **2005**, *11*, 873–888.

(38) Besora, M.; Lledós, A.; Maseras, F. *Chem. Soc. Rev.* **2009**, *38*, 957–966.

has been found. The protonation of **1** with HBF_4 leads to the metastable dihydrogen complex **3a**, which upon gradual H_2 loss generates what seems to be a coordinatively unsaturated species **3b**. In a similar fashion, the protonation of **2** with HBF_4 yields the isomeric cationic dihydrogen complexes **4a** and **4b**, which decompose at temperatures above $0\text{ }^\circ\text{C}$.

Acknowledgment. We thank the Ministerio de Ciencia y Tecnología (DGICYT, Project CTQ2007 60137/BQU) and Junta de Andalucía (PAI FQM188, P08-FQM-03538) for

financial support, and Johnson Matthey plc for generous loans of ruthenium trichloride.

Supporting Information Available: Tables of X-ray structural data, including data collection parameters, positional and thermal parameters, and bond distances and angles for complexes **1** and **2a/b**. This material is available free of charge via the Internet at <http://pubs.acs.org>.

OM900157B